

IMPEDANCE CALCULATIONS FOR THE NSLS-II STORAGE RING*

A. Blednykh[#], M. Ferreira, S. Krinsky
 BNL, NSLS-II, Upton, New York, 11973-5000, U.S.A.

Abstract

Impedance of two vacuum chamber components, Bellows and BPM, is considered in some detail. In order to avoid generation of Higher-Order Modes (HOM's) in the NSLS-II bellows, we designed a new low-impedance RF shielding consisting of 6 wide and 2 narrow metal plates without opening slots between them. The short-range wakepotential has been optimized taking into account vertical offset of RF fingers from their nominal position. The results were compared with data of bellows designed at other laboratories.

Narrow-band impedance of the BPM Button has been studied. TE-modes in the BPM button were suppressed by a factor of 8 by modification of existing housings. Two new types of housings are shown.

The total impedance of the NSLS-II storage ring is discussed in terms of the loss factor and the vertical kick factor for a 3mm-Gaussian bunch.

BELLOWS

Due to a large number of Regular Bellows (radius $r=12.5\text{mm}$) and ID Bellows ($r=5\text{mm}$) in the ring, it is important to design RF shielding with a low impedance. There are many different designs of bellows with thin copper (or stainless steel) fingers. We analyzed some designs of bellows developed at other laboratories for their impedance contribution. Impedance of these bellows depends on the number of slots between spring fingers, the slot width and the beam pipe radius. To design low-impedance RF shielding for the NSLS-II bellows we paid the main attention to:

- Location of the slots and their geometric dimensions.
- Generation of Higher-Order Modes (HOM's) inside the bellows due to slots between RF metal fingers.
- Vertical offset of RF spring fingers.

Location of the slots far away from the electron beam trajectory can reduce contribution to the wakefield and impedance. However electromagnetic fields generated due to slots can penetrate into the space between RF fingers and bellows. In this case, generated RF fields can be classified as modes like in a coaxial cavity with almost elliptical inner conductor. A big concern is that these modes can lead to heating of RF spring fingers and the bellows itself. To avoid generation of HOM in the NSLS-II bellows, we designed new RF contact fingers which are going to be made from 6 wide and 2 narrow metal plates fixed at both ends of the structure (Fig. 1) [1]. The RF Fingers designed so that there are almost no opening slots

between them and at the same time flexible to deformations. We believe that long-range wakepotential (Narrow-band impedance) analysis will show that due to very good contact between plates, we eliminate generation of HOM like those in a coaxial cavity. In Fig. 1, we show the real part of the longitudinal impedance ($\text{Re}Z_{||}$) if two narrow plates are missed horizontally. Strong narrow-band impedance is generated between 6 wide plates and bellows.

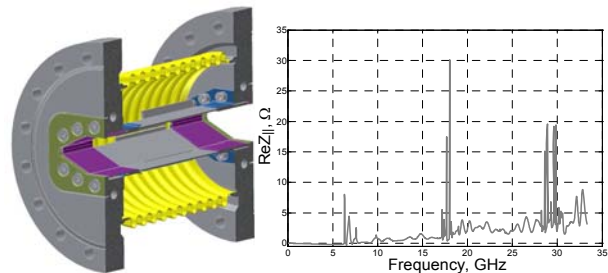


Figure 1: The NSLS-II RF shielded bellows.

Location of the RF metal fingers relative to the regular vacuum chamber (inside or outside) can play a significant role in producing the short-range wakepotential (broad-band impedance). The contribution of the bellows to the impedance needs to be analyzed in two cases: the worst misalignments of two consecutive vacuum chambers across the bellows and the straight positions. The main effect can be due to a small offset of the RF fingers from their nominal positions. The maximum offset allowed in the project is 2 mm in any direction.

The short-range wakepotential has been calculated with a 2mm vertical offset of RF fingers and with a vacuum chamber length of 500mm (Fig. 2). The length of 500mm was taken for simplicity. For example, the NSLS-II regular dipole vacuum chamber length is 2.6m.

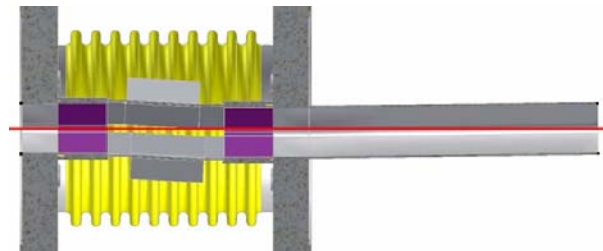


Figure 2: RF shielded bellows with a 2mm vertical offset.

In Table 1 we compare the loss factor for several geometries of bellows used at other laboratories. The loss factor is calculated for a 3mm Gaussian bunch in geometries with RF fingers at nominal position and with a 2mm vertical offset. Most of the models have reasonable low geometric impedance at a nominal position of spring

*Work supported by DOE contract DE-AC02-98CH10886.

[#]blednykh@bnl.gov

fingers. However the results are changed significantly by introducing a 2mm vertical offset (Table 1).

Due to a large number of the RF fingers and a small transition angle inside the APS bellows [2] the loss factor has a high value even at the nominal position of RF fingers ($\kappa_{loss}=64mV/pC$). The SPEAR3 bellows [3] with RF shielded fingers which extends the shape of the vacuum chamber inside the bellows shows a big effect on impedance value. It is almost similar to that shown for the APS bellows. Design of the SOLEIL bellows gives a small contribution to the impedance with 12 RF fingers [4]. The loss factor is increased by a factor of 4 with a 2mm vertical offset of RF fingers (Table 1). The loss factor for the NSLS-II design is comparable with data for the SOLEIL bellows at nominal positions of RF fingers and by a factor of 2 less for a 2mm vertical offset.

Table 1: Loss factor comparison for a 3mm Gaussian bunch.

Bellows	$\kappa_{loss}, mV/pC$	
	Nominal	Offset 2mm
APS	64	-
SOLEIL	20	86
SPEAR3	67	-
NSLS-II	18	37

BPM

Two types of BPM buttons, with diameters $\varnothing 7mm$ and $\varnothing 4mm$, are going to be used in the NSLS-II storage ring to determine position of the electron beam. Four $\varnothing 7mm$ buttons will be located on the elliptical multipole vacuum chamber (full vertical height of 25mm) referred to as the Regular BPM. Due to excitation of resonant modes in the buttons, the impedance, kick factor and loss factor depend strongly on the BPM button geometry. Some of the modes, H_{m1} -mode like in a coaxial waveguide, are trapped in a space between the housing for a button and the button itself [5]. Electromagnetic fields of these modes generated at multiples of the RF frequency can be accumulated inside the button due to passage of multi-bunch trains (equally spaced). As a result, these modes can cause additional power loss. The loss factor can be expressed as

$$\begin{aligned} \kappa_{loss} &= \sum_{n=0}^{\infty} \int_{-\infty}^{\infty} ds \int_{-\infty}^{\infty} ds' \rho(s) w(s'-s+nl) \rho(s') = \\ &= \sum_{n=0}^{\infty} \frac{c}{\pi} \int_0^{\infty} dk |\tilde{\rho}(k)|^2 [\text{Re} Z(k) \cos(knl) + \text{Im} Z(k) \sin(knl)] \end{aligned}$$

where l is the distance between bunches, Z is longitudinal impedance, w longitudinal wakepotential, ρ line-charge density and $\tilde{\rho}$ its Fourier transform. To avoid power losses due to coupled bunch effect, resonance frequencies of trapped modes have to be located away from frequencies multiple to the RF [6] or another way is to

damp higher order modes to attain the required level of quality factor (Q).

In this paper we present two new modified models of housings for the BPM button (Fig. 3b and Fig. 3c), which significantly reduce impedance and the quality factor of trapped modes. The regular button (electrode) has a T-shape form with a maximum radius of $r_1=3.5mm$ and with a minimum radius of $r_2=2.5mm$ (Fig. 3a, yellow color). The button is located in a cylindrical housing with a radius of $R_h=3.75mm$. The first lowest mode (H_{11} -mode) in this model is generated due to a passing bunch at frequency of $f_0=13.65GHz$ (Fig. 4, gray color). The cut-off frequency for H_{m1} -mode like in a coaxial waveguide can be defined as

$$f_c^{H_{m1}} \approx \frac{c}{\pi} \frac{m}{(r + R_h)}, \quad (1)$$

where r and R_h are the radii of the inner and outer conductors and $m=1,2,3,\dots k$. In a region where the T-shape button has a minimum radius ($r=r_2$) the H_{11} -mode has a cut-off frequency of $f_c^{H_{11}} = 15.3 GHz$. Due to higher cut-off frequency $f_0 < f_c^{H_{11}}$ in a space between r_2 and R_h this mode is trapped between button (r_1) and housing (R_h) and its field radiates into the beam channel.

The cut-off frequency for the H_{11} -mode can be reduced by increasing housing radius (from R_h to R_{hmax} , with fixed gap) and keeping button dimensions the same as shown in Fig. 3b. With a housing radius of $R_{hmax}=6mm$ (Cup-shaped housing) the cut-off frequency becomes $f_c^{H_{11}} = 10.1GHz$. For $f_0 > f_c^{H_{11}}$ numerical simulations show that the longitudinal wakepotential (Fig. 5, orange line) decays rapidly. The magnitude of the longitudinal impedance (Fig. 4, orange line) drops down by a factor of 5.

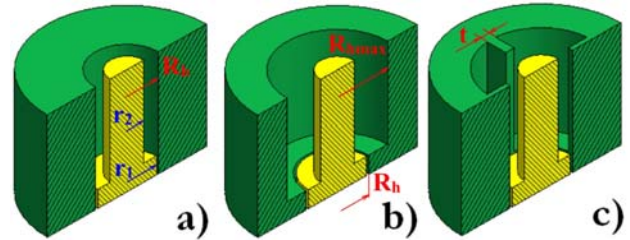


Figure 3: Housing modification for the BPM Button.

Another way to reduce the cut-off frequency in order to allow H_{11} -mode to propagate outside is to use a ridged housing (see Fig. 3c). For a thickness of $t=1mm$ and radius of $R_{hmax}=5.5mm$ the cutoff frequency is $f_c^{H_{11}} = 9 GHz$. In this case the magnitude of $ReZ_{||}$ becomes smaller by a factor of 8 ($ReZ_{||}=4\Omega$) and $W_{||}(s)$ at $s=400mm$ is almost zero (Fig. 4 and 5, blue color). The quality factor of the first damped mode is ~ 10 . Its damping time is $\tau=2Q/\omega=0.2ns$. For a bunch train with the bunch spacing time ($\tau_b=2ns$) $\tau_b > \tau$, HOM's generated at frequency close to harmonic frequencies cannot accumulate strong fields due to multiple bunch passages

and hence cannot provide additional heating. Hence losses in two considered cases will be predominantly due to the short-range wakepotential (single bunch effect) for both new proposed models.

Button modifications do not affect BPM resolution. The short-range wakepotential does not change for all three button geometries as it depends on geometric parameters such as: gap between housing and button, button diameter and button thickness [7].

For the numerical calculation “port” boundary condition was specified at the end of the button. Any further optimizations can be done with dielectric material instead of the port. A dielectric ring can be used both for vacuum insulation and for HOM damping. A real button has to be well matched to avoid reflection of propagating modes from a dielectric material.

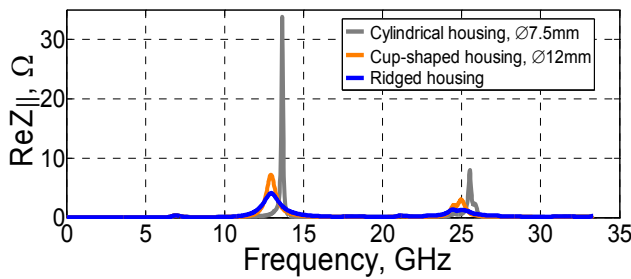


Figure 4: Real part of the longitudinal impedance.

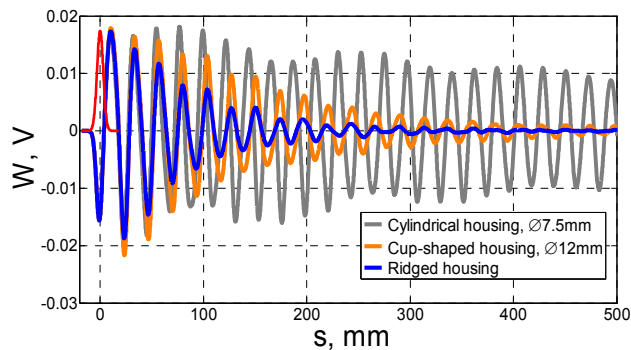


Figure 5: Longitudinal long range wakepotential.

NSLS-II IMPEDANCE ($\sigma_s=3\text{MM}$)

In Figure 6 and 7 are shown the contribution of the components of the NSLS-II storage ring in percentage values to longitudinal and transverse impedances. Significant contributors to the longitudinal impedance in terms of the loss factor are 651m aluminum surface with a 12.5mm radius (27%) and the tapers for the RF cavities (25%).

In-Vacuum Undulators with a half-gap of 2.5mm are crucial components in generating of the vertical impedance in terms of the kick factor. Their contribution is due to geometric impedance (37%) and resistive wall (36%). For 15 IVUs with a 2.5mm half-gap and each 3m length, 73% of the total kick factor is due to the IVU.

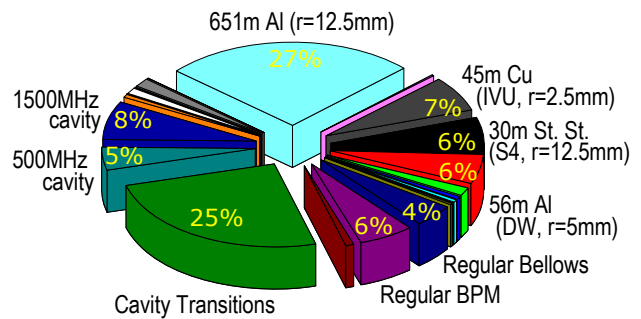


Figure 6: Contribution of the individual components and resistive wall effect to the loss factor for $\sigma_s=3\text{mm}$.

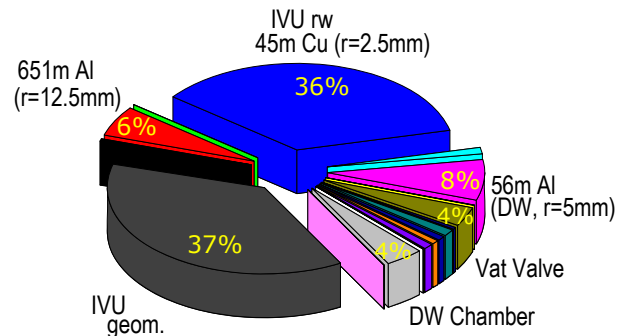


Figure 7: Contribution of the individual components and resistive wall effect to the vertical kick factor for $\sigma_s=3\text{mm}$.

CONCLUSION

A preliminary impedance budget for NSLS-II has been determined using a 3-mm driving bunch. The results obtained thus far are within the envelope of the model [8] we have used to estimate thresholds. Thus, we believe our estimations are conservative. We are working to complete the calculation of impedances for all vacuum components of the storage ring using the GdfidL code [9]. We are also working to calculate wakepotentials for bunches short compared with that of the stored beam to be used in TRANFT code [10] as pseudo-Greens function.

REFERENCES

- [1] L. Doom and M. Ferreira, private communication.
- [2] J. Jones et al., PAC99, p. 3095.
- [3] A. Trautwein, SLAC, private communication.
- [4] Synchrotron SOLEIL, <http://www.synchrotron.fr/portal/page/portal/SourceAccelerateur/Accelerateurs/SystemeVide>.
- [5] C.-K. Ng et al., PAC95, p. 2485.
- [6] P. Cameron et al., 'Button Optimization to Minimize Distortion due to Trapped Modes Heating' Proc. PAC09.
- [7] R. Nagaoka, EPAC'06, Scotland, p. 2850.
- [8] A. Blednykh and S. Krinsky, Proc. PAC07, p4321.
- [9] W. Bruns, GdfidL code; <http://www.gdfidl.de>
- [10] M. Blaskiewicz, "The TRANFT User's Manual version 1.0", BNL-77074-2006-IR, 2006.